JCBI
Journal of Computing & Biomedical Informatics
ISSN: 2710 - 1606
Volume 06 Issue 02
2024

Research Article
https://doi.org/10.56979/602/2024

Modified U-Net Model for Segmentation and Classification of Liver Cancer Using CT Images

Zunaira Naaqvi[1], Muhammad Ali Haider[2], Muhammad Rehan Faheem[3], Qurat Ul Ain[1], Amina Nawaz[4], and Ubaid Ullah[1*]

[1]Department of Computing, Riphah International University Faisalabad, Faisalabad, Pakistan
[2]Department of Artificial Intelligence, School of Systems and Technology (SST), University of Management and Technology, Lahore, Pakistan
[3]Department of Computer Science, The Islamia University of Bahawalpur, Bahawalpur, Pakistan
[4]Department of Computing, University of Agriculture, Faisalabad, Pakistan
[*]Corresponding Author: Ubaid Ullah. Email: ubaid.aleemisb2014@gmail.com

Received: March 23, 2023 **Accepted:** November 05, 2023 **Published:** March 01, 2024

Abstract: Liver cancer is becoming more common worldwide, and precise and accurate tumor segmentation is required for early detection. However, segmenting tumors is extremely difficult due to their hazy borders, variability in appearance, sizes, and varying densities of liver tumors. In the domain of medical images, a multimedia-based system is an ultimate requirement. It is a primary need in the healthcare industry that is also necessary for patients and doctors to achieve quick and efficient results. Deep learning-based approaches are currently being used to improve performance in various domains. Preprocessing, augmentation, segmentation, and classification are the four stages of the proposed framework. Because deep learning methods perform well on large datasets, the effects are evaluated of data augmentation synthetically and then used the five times transformation technique to increase the number of training samples. This paper proposes a deep-learning method for segmenting liver tumors based on a modified U-Net model called the AU-Net model. This framework employs an AlexNet CNN-based architecture to classify liver tumors. As a result, the 3D-ircadb01 and LiTs datasets were used, which are freely available. On the 3D-ircadb01 and LiTs datasets, the proposed architecture gained accuracies of 97.6% and 98.45% for liver classification. The proposed architecture consistently produces the best and most accurate results compared to other state-of-the-art methods.

Keywords: liver cancer; segmentation; U-Net; classification; AlexNet; convolutional neural network

1. Introduction

Globally, cancer is the second-most common cause of death. The World Health Organization (WHO) reported that it was the cause of 8.8 million deaths in 2015, with 788,000 of those deaths being related to liver cancer [1]. One of the two primary metabolic systems that comprise the human body is the liver, which is the largest parenchymal organ [2]. The abnormal growth of liver cells in the liver is known as hepatic cancer, or liver cancer. It makes up 2% of the body's mass and weighs close to 1.5 kg. It is essential to the metabolism of the body. The liver serves two physiological purposes: those of the hepatic sinusoids and those of the hepatocytes [3]. A World Health Organization (WHO) report indicates that 62.6% of human deaths result from liver diseases, with 54.3% of those caused by cirrhosis, and more than two-thirds of hepatitis cancer cases all over the world stem from this region [4]. In Asia, liver cancer type cirrhosis is the most common reason of death related to liver diseases, according to a WHO report. About 399,000 people died from liver diseases in 2016, such as cirrhosis, hepatitis, and hepatocellular carcinoma [5]. The WHO is working on a strategy to diagnose liver disease as a public health issue.

There has been a significant increase in liver cancer-related deaths in the past few years, and scientific contributions should control it. Primary cancers such as hepatocellular carcinoma or HCC cause 80% of all deaths [6]. Around 700,000 patients die yearly from primary cancers. Cirrhosis is the leading cause of primary liver cancer. It is usually due to alcohol consumption in the human body, hepatitis C and B viruses, or obesity resulting in liver disease. Computed tomography (CT) is the most common imaging test that helps diagnose cirrhosis, although ultrasound, MRI, and CT are also helpful [7]. A CT provides complete cross-sections of the abdominal area, which makes it a comprehensive test type. The homogeneity between the tumor and surrounding lesions can pose a challenge while segmenting CT scan images [8]. The result is not appropriate for liver tumor segmentation. So, for more accurate results, it's recommended to use enhanced images. By spotting a variation in the liver's pixel intensity, the CT scan locates the tumor [9]. The portion of the liver that is darker in color than the surrounding tissues is known as hypodense tissue.

Additionally, it has been observed that conventional tumor segmentation techniques take a long time to process [10]. A clinical situation, in this case, would not be ideal. It is normal for the human liver to exceed the maximum CT volume of 150 slices. The tumor and surrounding regions are also found to have a lot of irregularity in shape and low contrast [11]. To segment liver tumors from abdominal CT scans, researchers worldwide are working on Computer Aided Design (CAD) systems [12]. Because they relied on edge detectors, tumors cannot currently be segmented reliably and effectively. Convolutional Neural Networks (CNN) is one of the Deep Learning (DL) based algorithms that have been developed for automatic tumor segmentation [13]. As a widely used approach for segmenting liver tumors, CNN continues to attract the attention of most researchers.

In semantic segmentation, Forward Convolutional Neural Network (FCNN) is a more modified kind of CNN architecture. The semantic segmentation process works by assigning specific labels to every pixel in an image [14]. The Semantic segmentation architectures and other CNN architectures for image classification require semantic representations from the image input [15]. By boosting the convolution layers, these systems typically get rich contextual information. A convolution kernel needs receptive regions to receive contextual information. In that order, small- and large-scale features stay connected to tiny receptive fields. Convolution features never take contextual information into account, even though they fully observe region of interest (ROI) for specific receptive fields [16]. MRI or CT scans of liver tumors have shown incredibly thin lines and boundaries surrounding lesions, the result of years of research into liver tumor segmentation. It is challenging to accurately detect and segment tumors as a result of these issues. Therefore, having enough contextual data with better feature learning quality in terms of return on investment should be a requirement. Many researchers have worked on patch-based methods to deal with this situation [17]. These techniques convert the medical images into small patches and then segment them.

Similarly, many researchers have suggested better DL methods with improved feature learning for more accurate or better performance. However, few gaps can be filled with the improvement of the model's feature learning. Different researchers have proposed many end-to-end segmentation models, the most common of which is U-Net. Modified versions of U-Net have also been proposed for tumor segmentation [18].

This study focused on a medical diagnostic system that offers a complete solution to assist physicians. The proposed model name is AU-Net, the modified unit of the U-Net framework. Various researchers have used the U-Net technique for segmentation, but still, there is a feature learning gap that needs to be appropriately addressed. Therefore, this research used an improved U-Net model for tumor segmentation using CT images. The classification was performed using the AlexNet framework for more accurate and reliable results.

A model of liver tumors was made by integrating features from two different structures. To capture global context information from tumors of varying sizes, the first block used "parallel Atrous convolutions" using kernels to perform the input that operates simultaneously on the input. With Atrous convolutions, context can be obtained without introducing additional parameters, which in traditional convolutions are frequently increased since kernel sizes are large. The Atrous convolutions of various scales or dilations can function on input and simultaneously extract information from the image at various scales thanks to the parallel Atrous convolution structure. A specific issue has been addressed by the establishment of parallel structures.

Additionally, the result's feature maps were made more complex by applying Mish, a non-monoatomic smooth activation. The Mish activation function helps to easily control the overfitting problem in the model and has a very strong regularization effect. ReLu and Swish are inferior to this "activation function" since ReLu ignores negative feature map values. Moreover, all outgoing Weights connected to that node stay the same if ReLu activation is equal to 0 (zero). Hence, Mish activation, which also takes into account the significance of negative values in feature maps, does not operate in this manner.

Furthermore, the majority of these methods concentrate on tumor and liver segmentation. By comparison, this method is less complicated than tumor segmentation. On the other hand, the segmentation of the tumor is simple in the proposed method, and AlexNet was utilized for liver classification following the segmentation. Although it was a challenging task, the suggested AU-Net produced encouraging results. The performance of the suggested model was evaluated using the two publicly accessible databases, "3Dircadb and LiTs." Finally, a comparison was made between the suggested model's performance and that of current approaches. The major contribution of this research is as follows:

- AU-Net, an improved version of U-Net, effectively separates the tumor from the CT scan.
- Alex-Net is a classification architecture to classify small and irregular tumor areas.
- To deal with tumors of varying shapes and sizes, AU-Net employs a dilated multi-view kernel, and Atrous convolutions aggregate larger contexts at various CT scales in parallel.
- AU-Net incorporates res-blocks to address the issue of weight decay, while the training phase involves learning the residual mapping between convolution layers to generate tumor features.
- The Mish activation function, which has very strong regularization effects, adds nonlinearity to the network, improving both the original U-Net performance and interaction learning outcomes.

Furthermore, this paper is arranged as follows: Section 2 shows the literature for liver cancer segmentation and classification. Section 3 shows the proposed methodology in detail. The proposed model introduces the preprocessing, augmentation, segmentation, and classification methods used to classify liver cancer and its subtypes. Section 4 discusses the discussion and results. Finally, Section 5 of this study provides a conclusion and future directions.

2. Related Work

This section provides an in-depth discussion of current tumor segmentation methods. Tumor segmentation techniques have evolved over time, with some researchers adopting deep learning-based approaches and others sticking to more established methods. Using conventional methods, Elmenabawy et al. [19] proposed the use of CT images to segment liver and hepatic tumors, simultaneously and accurately automatically. These techniques separated extracted features using the deep learning neural network to control numerous liver tumors. For the experimentations, MICCAI'2017 and LITS challenge databases were used. The results show a DSC (dice similarity coefficient) of 93.5% for liver segmentation and 74.40% for tumor through the 5-fold cross-validation scheme.

Likewise, Kabe et al. [20] proposed a system for classifying liver tumors for hepatocellular carcinomas (HCC), metastases, lymphomas, and healthy tissues using two novel neural networks. During the first part, named FireNet, spatial features were extracted, while during another part, named MLstm, temporal information was gathered, and predictions were made. As a result of their experiments [20], A FireNet-MLstm network is 1.3 times lesser than a SqueezeNet-MLstm network, 76.6 times smaller than a ResNet network, and 16.6 times smaller than a GoogleNet network. FireNet-MLstm has fewer parameters than SqueezeNet-Lstm by 1.06 times, 82.5 times less than ResNet, and 10.1 times less than GoogleNet. It needs 2.3 seconds with 91.2% accuracy and performs better than other models.

Moreover, Nisa et al. [21] introduced an automated method for liver cancer detection that utilizes two methods: a conventional machine learning-based approach that leverages texture features and supervised learning to classify liver cancer. From 71 patients, almost 3000 CT scan image samples were obtained and clinically verified to determine if machine learning could correctly assess asymmetric patterns in CT images. However, the second algorithm identifies liver diseases based on semantic segmentation. Moreover, a convolutional neural network (CNN) is used to segment images using semantic image segmentation (SIS). The results showed the efficacy of the proposed model.

Furthermore, Wu et al. [22] suggested a model using multi-slice spiral computed tomography (MSCT) to diagnose liver cirrhosis and liver fibrosis using an artificial intelligence-based model. The study

comprised 112 patients in total. There were forty patients with mild fibrosis, forty-eight with significant fibrosis, and twenty-four with control scans. To de-convolve the images, the AI segmentation algorithm was run over them. The hepatic arterial fraction in the group with mild liver fibrosis was computed using the HAF test results. The average values of HAF, MTT, BF, and BV did not differ in a way that was statistically significant. Using an AI segmentation algorithm with MSCT imaging could improve the accuracy of liver cirrhosis and fibrosis diagnosis and open up new avenues for clinical diagnosis. Still, more research needs to be done on a single or small area for better results.

A prior study by Cao et al. [23] introduced a network that uses a CNN framework to perform motion detection (MD) and Sparse sinogram completion (SC). The x-ray tube voltage is gradually changed between three kVp levels, each of which covers a few degrees of gantry rotation. The feasibility of the slow kVp switching scheme was assessed through simulations with a liver-lesioned abdominal phantom. When compared to the ground truth, the line-integral SC network generated sinograms with a less than 0.05 RMSE of the line-integrals. It provided a passable quality of image up to nine degrees per kVp switchover angle. It ultimately distinguished between gadolinium and iodine in the sinogram domain as a result of MD network. The average relative quantification errors for both iodine and gadolinium were lower than 10%.

Another study by Al Sadeque et al. [24] proposed a method for treating liver cancer or malignant tumors that is based on the HOG-SVM algorithm. The stage before image preprocessing, ROI selection, and feature extraction using Histogram oriented Gradients (HOG) with CT images make up the method for detecting liver cancer. The noise in the images was separated using the median and Gaussian filters. The techniques used for image segmentation and liver area extraction were thresholding and countering. Moreover, the ROI-based Histogram Oriented Gradient (HOG) was used to extract features. When utilizing the machine learning SVM classifier, the suggested approaches showed 94% classification accuracy. There were 27 confirmed cases of liver cancer in the dataset.

Furthermore, Meng et al. [25] used Multiscale 3D (TDP-CNN) in the algorithm using LiTS as the dataset. The proposed model, which targets liver and tumors, was compared with other algorithms. Dice was 0.965 for segmentation and 0.689 for liver tumors, per the data.

Moreover, Fan et al. [26] developed a technique that uses CT scans and a deep learning (DL) classifier to identify liver and liver tumors. A collection of 131 liver CT scans that were made available to the public was used. Furthermore, this study uses Position-wise Attention Block (PBA) to capture spatial dependencies between pixels and Multiscale Fusion Attention Block (MFAB) to capture channel dependencies between features. The (MA-Net) model performed better than other methods in liver and tumor segmentation. To identify liver tumors on the public dataset, the dice value for the liver was 0.960 0.03, and the tumor segmentation was 0.7490.

A prior study by Das et al. [27] proposed an automatic model to detect cancerous regions on liver CT scan images by using spatial fuzzy clustering and adaptive thresholding. The public dataset's CT scan images were used. Spatial fuzzy clustering was utilized following the adaptive thresholding segmentation of the liver lesions affected by cancer. Following the division of the cancerous region, the features were removed and classified as types of liver cancer (HCC) and other cancers (MET). However, adaptive thresholding was used to keep the liver isolated from the kidney and spleen. The automated lesion segmentation process had finally come to an end. We used multilayer perceptron (MLP) and C4.5, two different decision tree classifiers, in conjunction with spatial fuzzy c-mean clustering. Both approaches detect the liver lesion successfully, with MLP 89.15 percent of the time and C4.5 classier 95.02 percent of the time.

Likewise, Das et al. [28] proposed a technique based on the Watershed model and the Gaussian Mixture Model (GMM). Two phases of the proposed method cancer lesion detection and liver separation were evaluated on a locally available dataset of 255 CT scans. After testing, the results show 100% sensitivity, 99.09% specificity, and 99.38% accuracy.

3. Materials and Methods

Method includes an analysis of this framework for liver cancer segmentation. A fully automated segmentation and classification methodology is presented in this section. Preprocessing, segmentation, and classification are the steps included in this framework. Additionally, the Figure 1 shows the suggested framework for liver cancer segmentation and classification flow diagram.

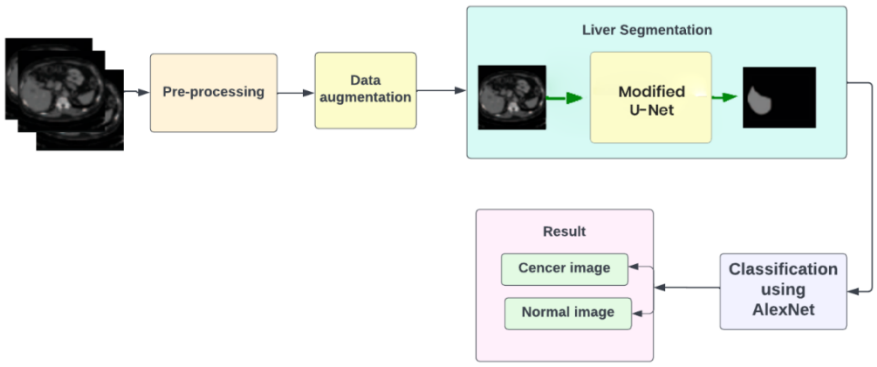

Figure 1. The process diagram of the suggested model

Dataset: Images are prepared from the two datasets to train and test the algorithm. According to the tumor's location on the liver, there are up to seven folders in 3D-ircadb01 [29] for each patient's tumor mask. Because the main aim is to segment the tumors, not to determine their anatomical placements, the liver cancer masks from diverse folders must be combined and placed in single folder. The LITS datasets have no separate masks for liver and tumor pictures, and the images are three-dimensional [30]. However, they can be found in the same segmentation folder under the same mask image. This algorithm contains 2D data, which should be converted to two-dimensional (2D).

Additionally, liver and tumor masks are separately created. The data was prepared using an image tool. Both files are stripped of the liver and tumor masks. To reduce the problem of class imbalance between the backdrop and foreground, the slices or pictures taken at the start and conclusion of the scanning liver data were removed from every patient.

Preprocessing: The goal of the suggested algorithm, AU-Net, is to extract tumors from the patient's CT scan picture. It is divided into three sections, these sections are the contracting path, a bottleneck path, and an expansive path. Figure 1 shows a graphic representation of the suggested AU-Net. The contracting path, which accepts input in the form of 256 x 256 x 1 CT slices, is where AU-Net starts to operate. The suggested AU-net block received the input. Atrous convolutions based on parallel structures and the Res block make up the RA block. To downscale an image, feature maps are fed into the size-pooling max-pooling procedure (2,2) after the RA-block. After each max-pool operation, a 0.05 dropout layer is added to control overfitting. However, figure 2 shows the liver's normal and enhanced CT Scan images for timely and efficient tumor detection.

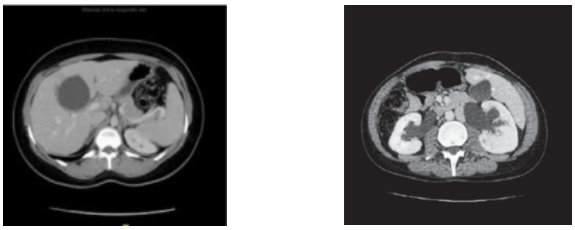

Normal CT image Enhanced CT image

Figure 2. Normal and Enhanced CT images of liver

Segmentation: The parallel structure based Atrous convolution block and the Res block receive the input from the RA block simultaneously. In the parallel Atrous convolution block, each 1 x 1, 2 x 2, and 3 x 3 Atrous convolution is used to gather more contextual data from various views. The gathering of tumor data on a range of sizes and scales is facilitated by this block. On the other hand, take into account a 2D input signal along with a feature map (x) and a kernel (w) weight matrix.

Bottleneck patch: The consequential feature maps are then passed to the bottleneck route after the input from the contracting route has been transferred. There is usually a layer with fewer nodes than previous layers in deep learning. In the neural network, the bottleneck is a layer with the fewest neurons, followed by layers before and after. This layer is used in deep learning to achieve a reduced dimensionality representation of the input. Bottlenecks are models that are forced to learn about the compression of inputs. The

bottleneck path in the proposed AU-Net model is an RA-block, and it consists of a residual module and parallel Atrous convolutions. The RA-block in the bottleneck path produces feature maps with a resolution of 16 x 16 x 1024 pixels. Other parameters that are the same as those used in the contracting path must be taken into consideration in addition to weight initialization, stride size, and padding parameters. All of the feature maps generated by this path are fed into the next expansive path as input.

Expensive Path: Results from the bottleneck patch is fed into the first 3 x 3 size transposed convolution layer, which the RA-block then follows. Moreover, the stride size in this convolution has been set, and the transposed convolution has been padded (2,2). The expansive path has four RA blocks, and four transposed convolution layers. Each transposed convolution layer is followed by a skip connection that connects the outputs of the expanding and contracting paths. This is achieved by concatenating the corresponding feature maps of the contracting path with the output feature maps of the transposed convolutions. More precisely, the output of the first transpose convolution layer of the expansive path and the output of the contracting path's final RA-block are concatenated. Moreover, three transpose convolution layers are reamed using the same procedure. This concatenation operation combines the image's contextual and localization data. Every RA-block in the expanding path has the following output dimensions: 32 x 32 x 512, 64 x 64 x 256, 128 x 128 x 128, and 256 x 256 x 64. Finally, a 1 x 1 convolution layer with sigmoid activation is used to create a segmented image. This 1 x 1 convolution maps the 64-component feature vector output of the previous RA-block to the number of classes supplied, tumor and background. Figure 3 displays the segmentation of the suggested model diagram.

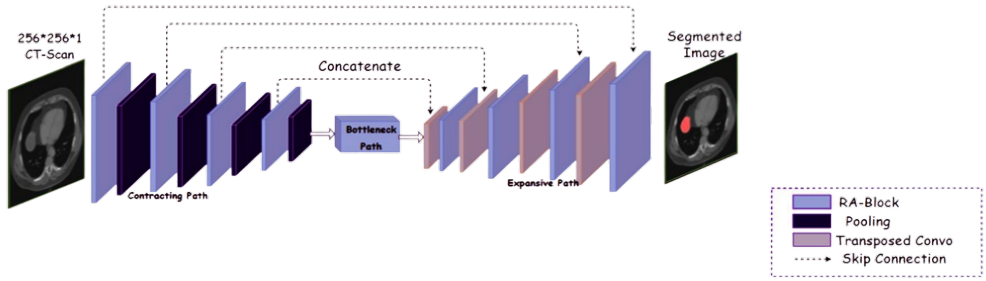

Figure 3. Shows modified U-Net model for segmentation of liver cancer.

Augmentation: On grayscale images, affine transformations such as translation, shearing, rotation, scaling, and flipping are the most often used augmentation techniques. Training errors must constantly decrease during the training phase to develop robust deep learning models. Enhancement/enrichment methods are used first to make this stage sustainable and cover a more comprehensive data point. By enabling different data transformations, image-based data enhancements enable a network generalization and improve its performance. Various methods have been described in the literature for increasing data. Some techniques include flipping, transferring, cutting, rotating, displacement, and adding noise. Among the widely used packages for data boosting is the Keras library. To increase data on images, the Keras library was used in this study [31]. The following operations were applied to data boosting: the range of rotation was 0.2, the range of width shift was 0.05, the range of height shift was 0.05, the range of zoom was 0.05, the range of horizontal flip was True, and the fill mode was 'nearest'. The datasets used for this study included 260 training and 50 test CT sections with the liver. The training and test sets have been quadrupled due to data boosting. This transformation technique applies five times to increase the large datasets for the proposed model. The sample size in the LiTs image bank and 3D-ircadb01datasets after data augmentation was 4886 and 5612, respectively.

Classification: After segmentation of the proposed model, the Alexnet architecture of CNN was used to classify CT images. During this phase, the Alexnet CNN network is used to classify LiTs and 3DIRCAD datasets. Using the pre-trained Alexnet, Advances in transfer learning techniques such as fine-tune layer and freeze layer have been substantial on liver cancer classification for their enhanced performance.

In object classification and reorganization applications, the AlexNet architecture of CNN is one of the best network architectures. There are eight layers in AlexNet, of which three layers are fully connected, and five layers are convolutional, before the first, second, and fifth convolutional layers for the

segmentation. On the other hand, Max Pooling layers have been integrated. Three and four convolutional layers are directly connected in this architecture. ReLU is the activation function that is used in all eight layers. In the final layer, for classification in every class, the SoftMax function is used to assign probabilities. A detailed description of the proposed AlexNet architecture can be found in figure 4.

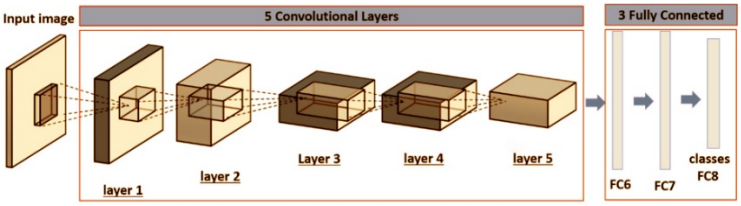

Figure 4. The classification of the proposed model using AlexNet architecture.

4. Results

This section defines the proposed framework outcomes for liver cancer classification. The Alexnet prediction accuracy for liver tumor efficient and accurate detection is 97.6%, recall 99.2%, F1 score 98.5% and precision98.99% using 3D-ircadb01dataset. However, the LiTs dataset attained an accuracy of 98.45%, F1 Score 97.88%, Recall 97%, and precision of 99.5%. On the 3DIRCADB dataset, based on the Jaccard score, the proposed framework provides an end-to-end solution for detecting tumors directly from CT scans and has a Jaccard score of 82%. And LiTs dataset has an encouraging Jaccard score of 89% with an end-to-end solution for detecting liver tumors using CT images. Table 1 shows the detailed results of the proposed architecture of both datasets for liver cancer classification. The graphical representation of the proposed model outcomes is illustrated in figure 5.

Table 1. Classification results of both datasets for liver cancer detection.

Dataset	Accuracy	Recall	F1-score	Precision
3D-ir-cadb01	97.6%	99.2%	98.5%	98.99%
LiTs	98.45%	97.88%	97%	99.5%

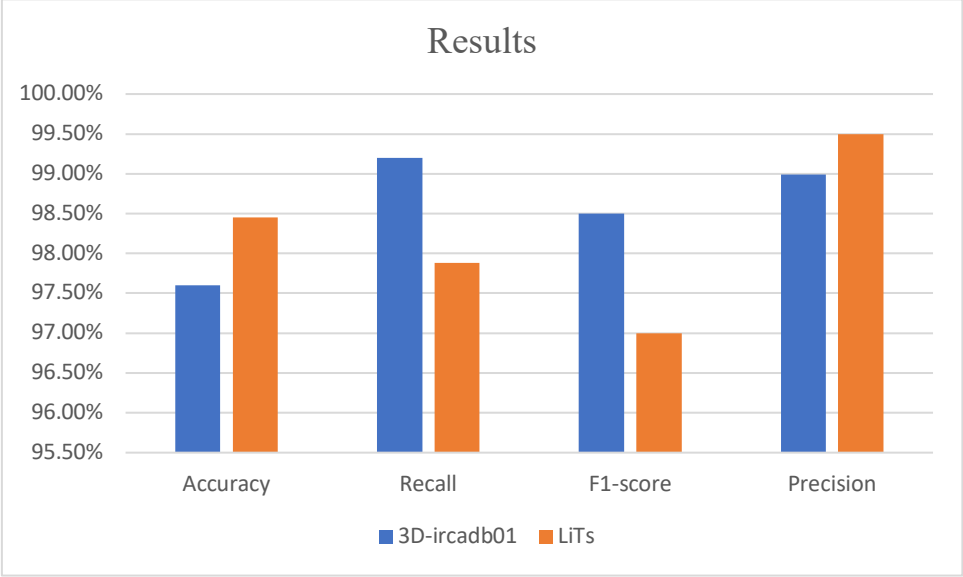

Figure 5. The graphical representation of Evaluation Parameters

5. Discussion

This study suggests a CNN-based deep learning technique for liver tumor segmentation. The Alexnet model is trained using transfer learning techniques to classify CT images, and preprocessing is performed to enhance the performance of the proposed model. The two primary phases of the suggested framework, segmentation and classification, enable quick and precise identification of liver cancer. The suggested technique needed a lot of data to be trained in order to yield complex and precise results. Thus, the binary classification model is trained and tested on two distinct datasets (3D-ircadb01 and LITS). On the website, there is an open-source 3D CT-scan imaging dataset called the 3D-ircadb01 database. You can use these databases for anatomy education or medical simulation. It includes ten images of women and ten images of men with liver tumors from 3D CT scans.

Moreover, The LiTs is a publicly available dataset of CT scan images of patients with liver cancer. An automated segmentation algorithm was developed by the researchers to differentiate liver lesions from CT images of the enlarged abdomen. Medical analysis and the diagnosis of treatable illnesses have been based on the most recent image release. The LITS dataset contains 130 CT scan images, including 70 test images. The pictures measured 512 by 512 pixels with a slice thickness between 0.7 and 5 mm. This chapter provides a brief explanation of how liver cancer detection and treatment can benefit from the application of AI techniques. As table 2 illustrates, deep learning technologies yield optimal results when applied to large datasets, which is why this transformation is performed five times to increase the number of images in publicly available datasets. Following data augmentation, 4886 and 5612 samples total were found for the 3D-ircadb01 and LiTs Image Bank datasets, respectively. The interconnected modules created using this suggested model form the foundation of the AlexNet CNN architecture. The suggested model seems to perform well in tumor regions with low contrast.

Table 2. The number of images before and after augmentation with their respective datasets.

Datasets	Type	Number of Images
3D-ir-cadb01	Before Augmentation	20
3D-ircadb01	After Augmentation	4886
LiTs	Before Augmentation	131
LiTs	After Augmentation	5612

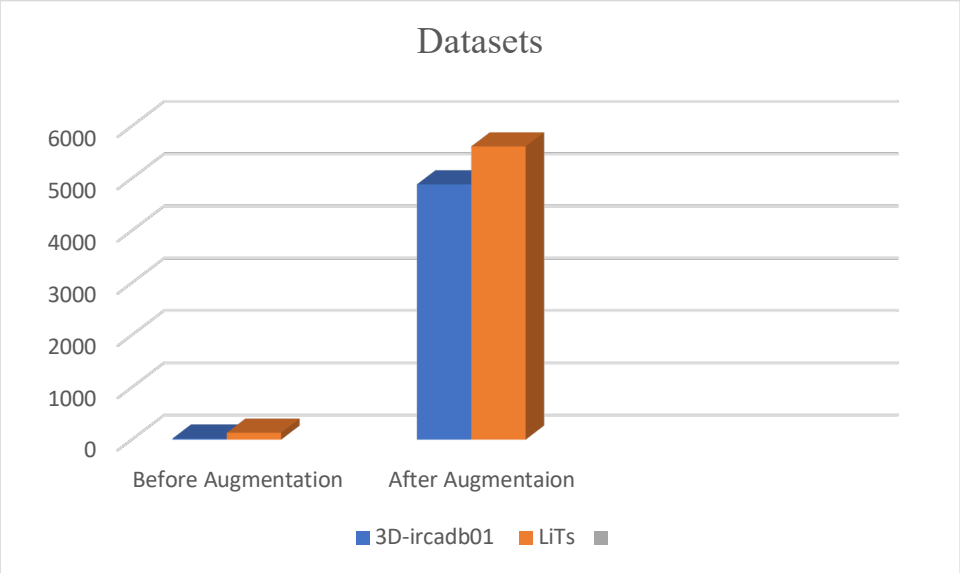

Figure 6. Before and after applying data Augmentation.

After the detailed analysis, it was discovered that the proposed model performed admirably and generated promising results. However, a comparison with some existing tumor segmentation methods should be carried out. This comparison shows that the proposed AU-Net model is useful for accurately

segmenting liver tumors. Various researchers proposed networks based on the resulting values of the liver tumor segmentation models. However, the proposed modified U-Net model is showing promising results.

Modified U-Net Segmentation: The outcomes and contrasts with current techniques show that the suggested unit successfully segments tumors. Tumors have heterogeneous features, including irregular sizes and shapes, which makes it challenging to use a segmentation algorithm to segment them, as was mentioned in the introduction. In this work, we propose a parallel Atrous convolution block that uses a parallel structure to extract features related to tumor size. This module's atrous convolutions capture different tumor sizes according to different dilations, scales, and sizes. The goal of the suggested block is to use various scale kernels to encode heterogeneous tumor features.

Furthermore, we used Atrous convolution to capture a wider context without increasing the number of parameters in the model, since standard convolution allows a 5 x 5 kernel matrix to have up to 25 parameters. With Atrous convolution, data is extracted from 5 x 5 image regions using a 3 x 3 kernel with just 9 parameters that come from dilation rates. Because it concentrates on a broader view/context, this approach broadens the model's receptive field while using fewer parameters. The performance of the model is also significantly influenced by the activation function.

The segmentation block makes use of a Mish activation function. Its regularization properties make it an excellent choice for the block. In particular, information loss could occur if the ReLu activation fails to update the weights from a neuron that the ReLu outputs zero values from. The information in the feature maps is preserved when Mish is used in place of ReLu. Moreover, if we improve the layer configuration of the architecture, overfitting and weight decay will result from the extra layers. Network degradation can be tackled by learning residual maps from feature maps derived from convolution layers. Three improvements to the U-Net are possible, and a logical conclusion is reached. The first challenge is accurately identifying features from heterogeneously sized tumors. The architectural level fixes for overfitting, decaying weights, and finding critical information in feature maps make up the second and third improvements. The architecture performs better because it can segment tumors more accurately and learn from them thanks to features. Furthermore, the suggested model separated cancers straight from CT scans. Additionally, it is imperative to acknowledge the constraints of architecture, such as its incapacity to segment small tumors.

Model Implementation: We used the Python programming language to implement our proposed architecture in this study. The model implementation uses TensorFlow (an open-source Python deep learning library). To train and validate the data, NVIDIA RTX 3090 GPU with 16 GB RAM was used with a Windows 64-bit CPU and a Core i7, 7th generation, M3-7Y30 processor on a Windows 64-bit CPU.

Performance Metrics: In this work, the effectiveness of the model in dividing and categorizing liver tumors is evaluated using the performance metrics listed below. Dice similarity coefficients (DSC), Jaccard scores, symmetric volume differences (SVD), specificity, and accuracy are further metrics included in this set.

1. Dice Similarity Coefficient (DSC)

$$\mathrm{DSC} = \frac{2TP}{2TP+FP+FN} \quad (1)$$

2. Jaccard Similarity Score (JSC)

$$JSC = \frac{TP}{TP+FP+FN} \quad (2)$$

3. Accuracy

$$Accuracy = \frac{TP+TN}{TP+TN+FP+FN} \quad (3)$$

4. Symmetric volume difference (SVD)

$$SVD = 1 - DSC \quad (4)$$

5. Specificity

$$Specificity = \frac{TN}{TN+FP} \quad (5)$$

6. Precision

$$\mathrm{Precision} = \frac{\mathrm{TP}}{TP+FP} \quad (6)$$

7. Recall

$$\mathrm{Recall} = \frac{\mathrm{TP}}{TP+FN} \quad (7)$$

8. F1 Score

$$\text{F1} - \text{score} = 2 \times \frac{Precision \times Recall}{Precision + Recall} \times 100 \quad (8)$$

All of the False Positives, True Positives, and False Negatives are represented by the letters on the scale TN, TP, FP, and FN in the above equations.

5.1 Future Work

The proposed model is suitable to assist doctors and clinicians with diagnosis decisions related to liver cancer disease based on the results of this research. Because of its effectiveness, it's a good option for real-time medical applications. Future research on evolutionary algorithms and reinforcement learning for liver cancer diagnosis is possible. Future research will employ a variety of deep learning techniques to produce liver cancer classifications that are more reliable and accurate. Using large and diverse training and testing datasets, the fusion will also be implemented on deep neural networks. There are various ways to address these challenges, such as enhancing small segmentation

6. Conclusions

For automated classification and segmentation of liver cancer, we suggest the DL-based AU-Net model. An enhanced and expanded version of the U-Net architecture is called AU-Net. Segmentation is applied after certain preprocessing steps to improve low-contrast CT images. CT image classification has been done using the CNN architecture AlexNet. The highest level of accuracy liver cancer detection algorithm was proposed and trained on two datasets (3D-ircadb01 and LiTs). The suggested AU-Net extracts tumor features concurrently by using Atrous convolutions and parallel residual modules. Atrous is able to obtain the Multi-view kernels through parallel structure-based convolution, which eliminates the need for additional parameters and allows for the extraction of broader context.

Additionally, the activation function directly affects the network's performance. The Mish activation is utilized in this work as opposed to a monoatomic one. Moreover, residual mapping combined with Atrous convolutions is learned by this model to extract tumor features. The model performs better and its feature learning process is improved when all these attributes are combined. CT images accurately and efficiently detect liver cancer using the proposed framework. Publicly available datasets were multiplied by two times using transformation techniques. CT scans are segmented using the modified U-Net model name (AU-Net) algorithm. Liver cancer is classified using the AlexNet architecture. The average accuracy of the experimental results was 97.6% and 98.45%, respectively. A comparison of the proposed methodology with existing models was conducted as well. The outcomes show that the suggested framework (AU-Net) outperforms the similar prior techniques. In the future, we plan to test this model on additional sizable tumor segmentation databases.

Conflicts of Interest: According to the authors, there is no conflict of interest in this study.

References

1. Napte, K.M.; Mahajan, A. Liver Segmentation and Liver Cancer Detection Based on Deep Convolutional Neural Network: A Brief Bibliometric Survey. Library Philosophy and Practice 2021, pp. 1-27.
2. Xiang, K.; Jiang, B.; Shang, D. The overview of the deep learning integrated into the medical imaging of liver: a review. Hepatology international 2021, 15, pp. 868-880.
3. Denbow, D.M. Gastrointestinal anatomy and physiology. In Sturkie's avian physiology, ed: Elsevier, 2015; pp. 337-366.
4. World Health Organization. Available online: https://www.who.int/publications/i/item/depression-global-health-estimates
5. Rahimian, J.; Wilson, T.; Oram, V.; Holzman, R.S. Pyogenic liver abscess: recent trends in etiology and mortality. Clinical infectious diseases 2004, 39, pp. 1654-1659.
6. Davis, G.L.; Dempster, J.; Meler, J.D.; Orr, D.W.; Walberg, M.W.; Brown, B. et al. Hepatocellular carcinoma: management of an increasingly common problem. In Baylor University Medical Center Proceedings, 2008; pp. 266-280.
7. Li, W. Automatic segmentation of liver tumor in CT images with deep convolutional neural networks. Journal of Computer and Communications 2015, 3, pp. 146, 2015.
8. Li, B.N.; Chui, C.K.; Chang, S.; Ong, S.H. A new unified level set method for semi-automatic liver tumor segmentation on contrast-enhanced CT images. Expert systems with applications 2012, 39, pp. 9661-9668.
9. Chlebus, G.; Meine, H.; Moltz, J.H.; Schenk, A. Neural network-based automatic liver tumor segmentation with random forest-based candidate filtering. arXiv preprint arXiv:1706.00842, 2017.
10. Kumar, S.; Moni, R.; Rajeesh, J. Automatic segmentation of liver and tumor for CAD of liver. Journal of advances in information technology 2011, 2, pp. 63-70.
11. Zhao, J.; Li, D.; Kassam, Z.; Howey, J.; Chong, J.; Chen, B. et al. Tripartite-GAN: Synthesizing liver contrast-enhanced MRI to improve tumor detection. Medical image analysis 2020, 63, p. 101667.
12. Kumar, S.; Devapal, D. Survey on recent CAD system for liver disease diagnosis. In 2014 International conference on control, instrumentation, communication and computational technologies (ICCICCT), 2014; pp. 763-766.
13. Trivizakis, E.; Manikis, G.C.; Nikiforaki, K.; Drevelegas, K.; Constantinides, M.; Drevelegas, A. et al. Extending 2-D convolutional neural networks to 3-D for advancing deep learning cancer classification with application to MRI liver tumor differentiation. IEEE journal of biomedical and health informatics 2018, 23, pp. 923-930.
14. Nawaz, H.; Maqsood, M.; Afzal, S.; Aadil, F.; Mehmood, I.; Rho, S. A deep feature-based real-time system for Alzheimer disease stage detection. Multimedia Tools and Applications 2021, 80, pp. 35789-35807.
15. Xia, K.; Yin, H.; Qian, P.; Jiang, Y.; Wang, S. Liver semantic segmentation algorithm based on improved deep adversarial networks in combination of weighted loss function on abdominal CT images. IEEE Access 2019, 7, pp. 96349-96358.
16. Kuo, C.L.; Cheng, S.C.; Lin, C.L.; Hsiao, K.F.; Lee, S.H. Texture-based treatment prediction by automatic liver tumor segmentation on computed tomography. In 2017 International Conference on Computer, Information and Telecommunication Systems (CITS), 2017; pp. 128-132.
17. Habib, A.B.; Akhter, M.E.; Sultaan, R.; Zahir, Z.B.; Arfin, R.; Haque, F. et al. Performance analysis of different 2D and 3D CNN model for liver semantic segmentation: a review. In International Conference on Medical Imaging and Computer-Aided Diagnosis, 2020; pp. 166-174.
18. Almotairi, S.; Kareem, G.; Aouf, M.; Almutairi, B.; Salem, M.A.M. Liver tumor segmentation in CT scans using modified SegNet. Sensors 2020, 20, p. 1516.
19. Elmenabawy, N.; El-Seddek, M.; Moustafa, H. E.D.; Elnakib, A. Deep segmentation of the liver and the hepatic tumors from abdomen tomography images. International Journal of Electrical and Computer Engineering, 2022, 12, p. 303.
20. Kashala Kabe, G.; Song, Y.; Liu, Z. FireNet-MLstm for classifying liver lesions by using deep features in CT images. Multimedia Tools and Applications 2021, pp. 1-17.
21. Nisa, M.; Buzdar, S.A.; Khan, K.; Ahmad, M.S. Deep Convolutional Neural Network Based Analysis of Liver Tissues Using Computed Tomography Images. Symmetry 2022, 14, p. 383.
22. Wu, L.; Ning, B.; Yang, J.; Chen, Y.; Zhang, C.; Yan, Y. Diagnosis of Liver Cirrhosis and Liver Fibrosis by Artificial Intelligence Algorithm-Based Multislice Spiral Computed Tomography. Computational and Mathematical Methods in Medicine, 2022, 2022.
23. Cao, W.; Shapira, N.; Maidment, A.; Daerr, H.; Noël, P.B. Hepatic dual-contrast CT imaging: slow triple kVp switching CT with CNN-based sinogram completion and material decomposition. Journal of Medical Imaging, 2022, 9, p. 014003.
24. Al Sadeque, Z.; Khan, T.I.; Hossain, Q.D.; Turaba, M.Y. Automated detection and classification of liver cancer from CT images using HOG-SVM model. In 2019 5th International Conference on Advances in Electrical Engineering (ICAEE), 2019; pp. 21-26.
25. Meng, L.; Tian, Y.; Bu, S. Liver tumor segmentation based on 3D convolutional neural network with dual scale. Journal of applied clinical medical physics 2020, 21, pp. 144-157.
26. Fan, T.; Wang, G.; Li, Y.; Wang, H. Ma-net: A multi-scale attention network for liver and tumor segmentation. IEEE Access 2020, 8, pp. 179656-179665.
27. Das, A.; Das, P.; Panda, S.; Sabut, S. Detection of liver cancer using modified fuzzy clustering and decision tree classifier in CT images. Pattern Recognition and Image Analysis 2019, 29, pp. 201-211.
28. Das, A.; Acharya, U.R.; Panda, S.S.; Sabut, S. Deep learning based liver cancer detection using watershed transform and Gaussian mixture model techniques. Cognitive Systems Research 2019, 54, pp. 165-175.

29. Ircad France. Available online: https://www.ircad.fr/research/data-sets/liver-segmentation-3d-ircadb-01/ (accessed on 30-4-2022).
30. Codalab. Available online: https://competitions.codalab.org/competitions/17094 (accessed on 30-4-2022).
31. Frid-Adar, M.; Klang, E.; Amitai, M.; Goldberger, J.; Greenspan, H. Synthetic data augmentation using GAN for improved liver lesion classification. In 2018 IEEE 15th international symposium on biomedical imaging (ISBI 2018), 2018; pp. 289-293.